Journal of Fluorescence, Vol. 1, No. 4, 1991

Fluorescence Lifetime-Enhanced Spectral Characterization of Human Serum

Robert D. Stevens,[1] Michael S. Cooter,[1] and Linda B. McGown[1,2]

Received September 5, 1991; revised February 6, 1992; accepted February 7, 1992

Frequency-domain fluorescence lifetime techniques were used for the characterization of pooled human serum, including normal serum, hyperlipid serum, and sera that had been stripped of various components. Fluorescence lifetime measurements of normal human serum revealed lifetime components primarily in the regions of 10^2 ps, 1–2 ns, 4–7 ns, and 9–10 ns. Phase-resolved fluorescence spectroscopy (PRFS), a frequency-domain technique that combines spectral and lifetime information in measurements of phase-resolved fluorescence intensity (PRFI), provided the basis for comparison of the various sera. Measurements of PRFI vs excitation wavelength and emission wavelength yield a phase-resolved excitation–emission matrix (PREEM) at a given modulation frequency. Multifrequency measurements yield a three-way excitation–emission–frequency array. The multifrequency PREEMs of the various sera were compared with each other and with the corresponding two-way excitation–emission matrices (EEMs) that are obtained using conventional, steady-state fluorescence spectroscopy. Application of matrix-based analysis techniques to the steady-state and PRFS data arrays allowed direct comparison between the two approaches. Results demonstrate the enhanced discrimination among samples that is achieved through the additional dimension of fluorescence lifetime in PRFS.

KEY WORDS: Human serum; fluorescence lifetime; phase-resolved fluorescence spectroscopy; total luminescence.

INTRODUCTION

Fluorescence spectroscopy offers a uniquely powerful combination of advantages for chemical analysis, including high sensitivity, excellent detection limits, relative simplicity, and minimal sample preparation. It is particularly well suited to the characterization of complex, multicomponent samples since fluorescence measurements can be made directly on the intact sample without compromising the integrity of the sample matrix, thus preserving the full uniqueness of individual samples. This type of dynamic, physicochemical information about the sample is not available from separation-based techniques that employ chromatography or extraction to remove the components from the sample matrix.

Multidimensional fluorescence techniques based on the independent dimensions of excitation and emission spectra have been heavily exploited in recent decades through techniques such as total luminescence and synchronous excitation luminescence [1]. Such techniques have been used for the characterization of biological fluids, including human serum, serum ultrafiltrate, and human urine [2–4]. Fluorescence changes in the sera of cancer patients with certain types of tumor activity have also been investigated as a possible means for clinical detection and diagnosis [5,6]. Steady-state approaches to characterization of biological fluids are limited, however, by spectral similarities among samples. This is particularly true for human serum, in which the basic

[1] Department of Chemistry, P. M. Gross Chemical Laboratory, Duke University, Durham, North Carolina 27706.
[2] To whom correspondence should be addressed.

1053-0509/91/1200-0235$06.50/0

similarities among different samples far outweigh the relatively small differences.

The addition of the independent dimension of fluorescence lifetime greatly increases the information content of fluorescence measurements. Since fluorescence lifetime is a dynamic parameter, it will vary even for a single compound if the molecules of that compound are distributed among more than one dynamic microenvironment in a sample. Such microenvironmental heterogeneity may arise from aggregation and complexation processes, as well as from the presence of multiple binding sites in macromolecular structures such as lipid aggregates and proteins. Furthermore, fluorescence lifetimes will be affected by collisional processes such as quenching, energy transfer, and excited-state complex formation. These processes may occur at different rates in different microenvironments, due to variations in proximity and accessibility of the interacting molecules.

Phase-resolved fluorescence spectroscopy (PRFS) [7–9] is a commercially available, frequency-domain fluorescence lifetime technique which combines the multiple dimensions of excitation and emission spectral information with lifetime information, thereby taking full advantage of the high sensitivity of the fluorescence process to the microenvironment of the emitting molecules. By varying the frequency at which the intensity of the excitation beam is modulated, individual fluorescence spectral features in PRFS can be relatively enhanced or suppressed as a function of fluorescence lifetime. PRFS has previously been applied to the characterization of complex fossil fuel samples, including crude oils [10] and petrolatums [11].

This paper describes the first application of PRFS to the characterization of human serum. Measurements of fluorescence in the near-UV/visible region were made for commercial preparations of pooled sera, including normal serum, hyperlipid serum, and sera that were stripped of various components. All contributions from scattered light were suppressed through the appropriate adjustment of the detector phase, allowing measurements to be made of serum that was diluted only onefold with buffer. Minimal sample dilution maximizes the fluorophore concentration, which is important for measurements of the weak signals associated with visible fluorescence in serum, and minimizes the perturbation of the native sample matrix. Chemometric techniques were used for data analysis and noise reduction.

PRFS offers several advantages relative to other lifetime approaches that are currently available on commercial instruments. Because PRFS can be performed in a picosecond domain with a continuum source such as the xenon arc lamp used in this work, excitation scanning is readily performed. PRFS determinations do not require any more time or effort than the analogous steady-state determinations; a phase-resolved fluorescence intensity (PRFI) is measured in the same time (essentially instantaneously) and manner as a steady-state intensity. In this work, the PRFS and steady-state data were collected using the same instrument under identical conditions, aside from the excitation intensity modulation and phase-sensitive detection in the PRFS measurements, so that the performance of the two techniques is readily compared. Like steady-state intensities, PRFI signals of individual, independently emitting components in mixtures are additive. Thus, PRFI can be treated in a manner that is completely analogous to the treatment of steady-state intensity, using direct extensions of instrumental approaches and data analysis techniques that have already been developed for steady-state fluorescence.

THEORY

In PRFS [7–9], the sample is excited with a continuous beam of light of wavelength λ_{ex} that is intensity-modulated at a high frequency (f), typically in the megahertz range. The intensity of the excitation beam is therefore comprised of a sinusoidal (ac) component superimposed on a steady-state (dc) component:

$$E(t) = A + Am_{ex}\sin\omega t \quad (1)$$

where $E(t)$ is the total intensity at time t, A is the steady-state (dc) intensity, ω is the angular modulation frequency ($\omega = 2\pi f$), and $Am_{ex}\sin\omega t$ is the time-dependent (ac) component of the beam. The modulation depth, m_{ex}, is the ratio of the ac amplitude to the dc intensity.

Due to the finite lifetime of the excited state of the emitting species, the fluorescence emission at wavelength λ_{em}, $F(t)$, will be phased-shifted by an angle ϕ and demodulated by a factor m relative to the exciting light:

$$F(t) = A' + A'm_{ex}m\sin(\omega t - \phi) \quad (2)$$

where A' is the steady-state (dc) emission intensity. The fluorescence lifetime, τ, can be calculated from both the phase shift, ϕ,

$$\tau = (1/\omega)\tan\phi \quad (3)$$

and the demodulation, m,

$$\tau = (1/\omega)[(m^2)^{-1} - 1]^{1/2} \quad (4)$$

In PRFS, the ac component of $F(t)$ is multiplied by a periodic square-wave function, $P(t)$, of frequency ω that alternates between two values (0 and 1 on the in-

strument used in this work). The product of these signals is integrated over time to produce a phase-resolved fluorescence intensity (PRFI), which is a time-independent function of the spectral and lifetime characteristics of the emitting components:

$$\text{PRFI} = A' m_{ex} m \cos(\phi_D - \phi) \quad (5)$$

The detector phase angle, ϕ_D, is the phase of $P(t)$, which can be adjusted to any value between 0 and 360°.

Substituting for m and ϕ in terms of τ and ω [from Eqs. (3) and (4)] yields [12]

$$\text{PRFI} = A' \left(\{\cos[\phi_D - \tan^{-1}(\omega\tau)]\} / [(\omega\tau)^2 + 1]^{1/2} \right) \quad (6)$$

As shown by Eq. (6), PRFI retains the concentration and spectral dependence of the steady-state intensity (A') and adds the fluorescence lifetime dependence of the dynamic component of the emission signal. The PRFI for a particular lifetime component ranges from a maximum value when ϕ_D is set to be in phase with the fluorescence signal to the minimum value of zero when ϕ_D is exactly 90° out of phase with the fluorescence signal. In addition, the PRFI is also a function of ω, so that there are two independent instrumental parameters that can be simultaneously used to exploit fluorescence lifetime selectivity. Combined with λ_{ex} and λ_{em}, there is a total of four instrumental parameters (λ_{ex}, λ_{em}, ω, and ϕ_D) that can be controlled in the PRFS experiment, in order to exploit fully the multiple dimensions of fluorescence information.

Fluorescence lifetime selectivity afforded by PRFS can be thought of as a filtering process, in which intensity contributions from components inside a given lifetime range are selectively enhanced relative to those outside the range [13,14]. Thus, the spectral features of the individual components do not change, but their relative contributions to the total signal are enhanced or suppressed as a function of their fluorescence lifetimes. The lifetime range of the filter is determined by ω and the shape of the filter is determined by ϕ_D [14]. In this work, as in previous studies [10,11,15], the detector phase angle ϕ_D was set to suppress the contribution of scattered light ($\phi_D = \phi_{scatter} \pm 90°$) in each PREEM, thereby creating a "bandpass lifetime filter."

Conventional, steady-state fluorescence spectral data can be represented in a two-way data array, or excitation–emission matrix (EEM), in which intensity is plotted as a function of λ_{em} and λ_{ex} to generate a three-dimensional surface [16,17]. Fluorescence lifetime has been incorporated in the EEM in both time-domain [18] and frequency-domain [19] experiments, thereby extending the EEM into a fourth dimension. In the frequency-domain approach [19], PRFS is used to generate a phase-resolved EEM (PREEM), in which PRFI is plotted as a function of λ_{em} and λ_{ex} at each of several frequencies to produce a three-way, excitation–emission–frequency array (EEFA). The PRFI at each λ_{em}, λ_{ex} point in the EEFA varies along the frequency axis according to Eq. (6).

EXPERIMENTAL

All of the experiments were performed on commercial preparations of pooled human serum, including normal human serum (NHS), hyperlipid human serum (HHS), steroid-free human serum (SFHS), and testosterone-free human serum (TFHS). Lipid-stripped (ls) preparations of several sera, including NHS(ls), SFHS(ls), TFHS(ls), and thyroid stimulating hormone-free human serum [TSHFHS(ls)], were also studied. The sera were all used as received with no further pretreatment. Testosterone and phosphate-buffered saline (PBS) were obtained from Sigma Chemical Co. The PBS buffer solution (0.010 *M*, pH 7.4) was prepared in HPLC-grade deionized water and stored under refrigeration.

Serum samples were prepared for measurement by diluting 1.50 ml of the serum with 1.50 ml of PBS in cuvette. For experiments involving the addition of testosterone to testosterone-free serum, 0.2 mg of testosterone was dissolved in 2.00 ml of the serum and the solution was sonicated for 30 min. The resulting serum solution was then diluted with PBS in cuvette as described above.

All steady-state and phase-resolved spectra were collected using a multifrequency SLM 48000S phase-modulation spectrofluorometer with hardware-based phase resolution. The instrument incorporates a 450-W xenon arc lamp as the excitation source, excitation and emission monochromators for wavelength selection, a Pockel's cell for modulation of the excitation beam intensity, and conventional or phase-sensitive detection with a photomultiplier tube (PMT). A Haake A81 temperature control unit was used to maintain the temperature of the sample compartment at 20.0 ± 0.1°C. Quartz cuvettes were used for all measurements.

Each fluorescence intensity (steady state or phase resolved) was measured as the average of 10 samplings taken over a period of 3 s, performed internally by the instrument. Unless otherwise noted, PREEMs and steady-

state EEMS were collected with a scanning interval of 4 nm over a spectral region of λ_{ex} = 310–470 nm and λ_{em} = 380–540 nm, to generate 40 × 40 matrices of steady-state intensity or PRFI as a function of λ_{ex} and λ_{em}. The entrance and exit slits were set at 16/2 and 16/8 nm for the excitation and emission monochromators, respectively. In the initial studies of NHS, PREEMs were collected at six modulation frequencies: 115, 85, 25, 18, 10, and 8 MHz. Four of these frequencies, 115, 85, 25, and 10 MHz, were then selected for subsequent studies. All PRFS measurements were made with the detector phase angle ϕ_D set to suppress scattered light ($\phi_D = \phi_{scatter} \pm 90°$), using a kaolin scattering solution. Blank subtraction was not performed for any of the spectra. Since these are measurements of intrinsic luminescence, there is no relevant blank other than the buffer, which did not contribute any significant luminescence.

Software from SLM Instruments, Inc., and macro programs written in-house were utilized on an IBM PC-XT microcomputer for data acquisition and analysis. Additional chemometric analysis was performed on IBM PC-AT, HP 9920U, and Zeos 486 microcomputers. Surfer Software (Golden Software, Inc., Golden, CO) was used to generate the contour plots.

Fluorescence lifetimes were determined from heterogeneity analysis of phase-modulation data collected at five frequencies (5, 10, 25, 70, and 115 MHz), using nonlinear least-squares software provided with the 48000S instrument.

RESULTS AND DISCUSSION

The Total Fluorescence of Human Serum

Human serum is composed of a wide variety of components, only a few of which make significant contributions to the overall fluorescence. The total fluorescence of human serum can be divided into two characteristic regions [5]: a highly fluorescent UV region, 270–370 nm; and a near-UV/visible region, 390–580 nm. The UV region is dominated by one peak at λ_{ex} = 296 nm, λ_{em} = 336 nm, resulting from the strong fluorescence of proteins, primarily from tryptophan. The fluorescence of tyrosine in this region is generally negligible due to energy transfer to tryptophan.

Fluorescence of human serum in the near-UV/visible region is characterized by much weaker intensities, exhibiting two or three major peaks depending on the sample and instrumental factors [2]. The main fluorescent species in this region have been tentatively identified in the literature as NADH, NAD(P)H, pyridoxic acid and its derivatives, hydroxyanthranilic acids, riboflavin, flavin mononucleotide (FMN), and protein-bound bilirubin [2]. Contributions from low-density lipoproteins (LDLs) have also been reported [20].

Steady-State Excitation–Emission Matrices

Figure 1 shows the steady-state EEMs of each of the different types of pooled serum. The EEMs are all very similar, each dominated by a peak around λ_{ex} = 350 nm, λ_{em} = 440 nm. A second, intense peak in the lower left-hand corner in the EEM of NHS is attributed to protein luminescence. Sera that were stripped of a particular component exhibited lower fluorescence intensities than NHS and were measured at a higher applied voltage, which accounts for the appearance of the Raman peak of water (λ_{ex} = 348 nm, λ_{em} = 395 nm) in their spectra. The relatively minor differences between the steady-state spectral features, due primarily to small shifts in the position and orientation of the central peak, do not provide a strong or detailed basis for discrimination between the different sera.

Improvement of Signal-to-Noise Ratios in PREEMs

Signal-to-noise ratios for a given sample are lower for PRFS than for the corresponding steady-state intensity measurements, due to attenuation of the incident beam by the modulation optics and to the PRFS detection process. In this work, the noise contribution to each PREEM was reduced by using postacquisition data analysis. First, each PREEM was decomposed into its eigenvectors and corresponding eigenvalues by singular value decomposition [21,22]. Canonical correlation was then performed between PREEMs collected at different frequencies for a given sample in order to obtain an estimate of the rank **n** for the PREEMs of that sample [23]. For all of the pooled sera, **n** was estimated to be 3 and each PREEM was therefore constructed from the first three eigenvectors (i.e., those with the largest eigenvalues, which would correspond to the primary eigenvectors in a better-defined system). In order to be consistent, rank 3 constructions of the steady-state EEMs were used in quantitative comparisons of steady-state data.

Figure 2 shows contour plots of spectral data for NHS, including a steady-state EEM (raw data), a PREEM collected at 25 MHz (raw data), and a rank 3 PREEM constructed from the decomposed 25-MHz data. Visual examination of the rank 3 constructed PREEM reveals the presence of two major peaks: λ_{ex} = 366 nm, λ_{em} = 448 nm and λ_{ex} = 398 nm, λ_{em} = 468 nm. These peaks are referred to hereinafter as Peaks I and II, respectively. A

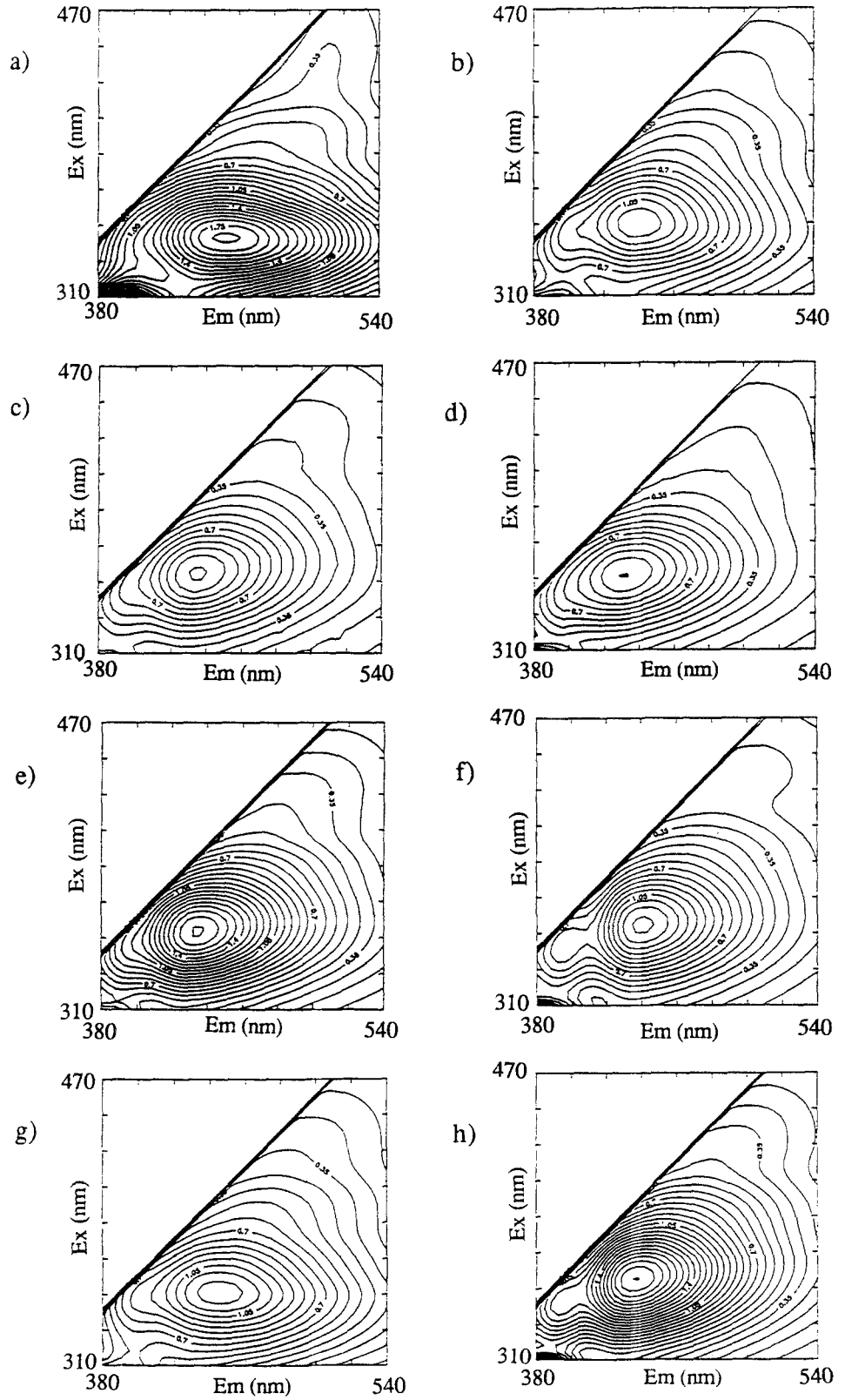

Fig. 1. Contour plots of steady-state EEMs of (a) NHS, (b) NHS(ls), (c) TFHS, (d) TFHS(ls), (e) SFHS, (f) SFHS(ls), (g) HHS, and (h) TSHFHS(ls).

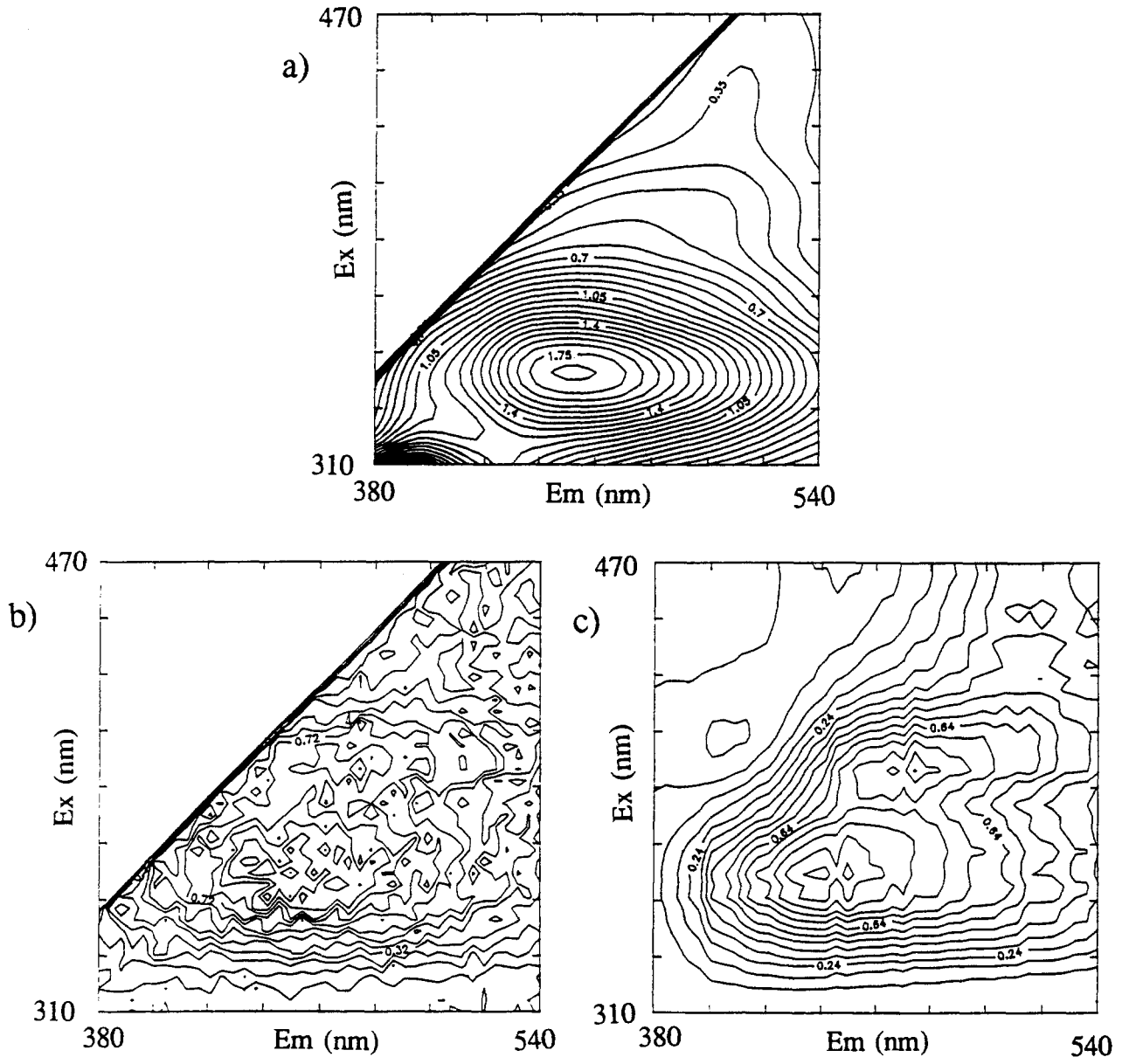

Fig. 2. EEM and PREEMs of NHS: (a) steady-state EEM, (b) PREEM at 25 MHz (raw data), and (c) rank 3 construction of 25-MHz PREEM.

weaker peak is also evident around $\lambda_{ex} = 446$ nm, $\lambda_{em} = 516$ nm.

Reproducibility of the EEMs and PREEMs for Normal Serum

Steady-state EEMs and PREEMs at 10, 25, 85, and 115 MHz were collected for various NHS samples, including (i) duplicate runs of the same sample (same lot, from Scantibodies), collected under identical conditions on 2 consecutive days, (ii) one run of a sample from a different lot from the same vendor, and (iii) one run of a sample from a different vendor (Chemicon Inc.). Uncorrected matrix correlations (UMCs) [22] were calculated between each of the three replicate EEMs or PREEMs for each sample from Scantibodies. The UMCs were

then averaged to obtain a single, mean UMC for the steady-state EEMs and the PREEMs at each frequency for NHS. The mean UMC values and standard deviations are shown in the first row of Table I.

The second row of data in Table I shows the mean UMCs for the NHS sample from Chemicon with the NHS standard from Scantibodies. There is less than 80% confidence of a significant difference between the samples, indicating that the EEMs and PREEMs for NHS from different vendors are indistinguishable.

In a separate experiment, five PREEMs were collected consecutively at a single frequency for a single sample (from Scantibodies), thus exposing the sample to several hours of continuous irradiation. The effects of such prolonged irradiation of the samples were found to be negligible.

Effect of Modulation Frequency

At each modulation frequency ω, the PRFI is maximized for components with $\tau = 1/\omega$. According to Eq. (6), the contributions of longer-lived species are enhanced at low frequencies and the contributions of shorter-lived species are enhanced at high frequencies. The modulation frequencies used in this study were chosen to cover a broad range of fluorescence lifetime ($1/\omega$ = 1.4 to 16 ns, which provides an effective measurement range of 10^{-1}–10^{1} ns).

Figure 3 illustrates the frequency dependence of the spectral features in the PREEMs of NHS. A clear progression is seen from a PREEM dominated by Peak I at 8 MHz, indicating a relatively long-lived fluorescent component, to a PREEM dominated by Peak II at 115 MHz, indicating a relatively short lifetime component. The relative contribution from the peak at $\lambda_{ex} = 446$ nm, $\lambda_{em} = 516$ nm in NHS is greatest at 115 MHz, which is consistent with the short (subnanosecond) fluorescence lifetime of protein-bound bilirubin [24]. The presence of two major fluorescence peaks with significantly different lifetimes in the PREEMs of normal human serum offers more detailed information than the single, dominant peak in the steady-state EEMs.

Comparison of PREEMs of Eight Pooled Sera

Figure 4 shows the PREEMs of each type of serum, collected at 85 MHz. This frequency was found to afford

Table I. Uncorrected Matrix Correlations (UMC) for NHS Replicates and for Various Pooled Sera with Normal Sera[a]

	UMC[b,c]				
Serum	SS	10 MHz	25 MHz	85 MHz	115 MHz
Standard: NHS					
NHS[d]	0.9955 (±0.0055)	0.9879 (±0.0047)	0.9896 (±0.0038)	0.9842 (±0.0026)	0.9838 (±0.0014)
NHS[e]	0.9938	0.9832	0.9859	0.9828	0.9813
TFHS	0.9071***	0.9518**	0.9735*	0.9269***	0.9337***
TFHS(ls)	0.9059***	0.9325***	0.9488***	0.9519***	0.9661***
SFHS	0.9045***	0.9546**	0.9721*	0.9640**	0.9718***
SFHS(ls)	0.9200***	0.9529**	0.9705*	0.9672**	0.9704***
NHS(ls)	0.9276***	0.9715*	0.9775*	0.9669**	0.9703***
HHS	0.9294***	0.9815	0.9771*	0.9735*	0.9724**
Standard: NHS(ls)					
SFHS(ls)	0.9886	0.9906	0.9925	0.9906	0.9876
TFHS(ls)	0.9888	0.9824	0.9857	0.9915	0.9909
TSHFHS(ls)	0.9879	0.9887	0.9931	0.9904	0.9877

[a] Steady-state (SS) EEMs and PREEMs are rank 3 constructions.
[b] UMC values calculated for various "test" sera with NHS or NHS(ls) standard.
[c] Significant difference between test and standard NHS sera indicated by superscript asterisks. Significance was not calculated for UMCs of lipid-stripped test sera with NHS(ls) standard due to lack of replicates for NHS(ls).
[d] Mean UMCs ± SD, calculated between triplicate EEMs and between triplicate PREEMs of NHS standard.
[e] UMC for NHS from different vendor as "test" with NHS standard.
* At 95% confidence level.
** At 99% confidence level.
*** At 99.5% confidence level.

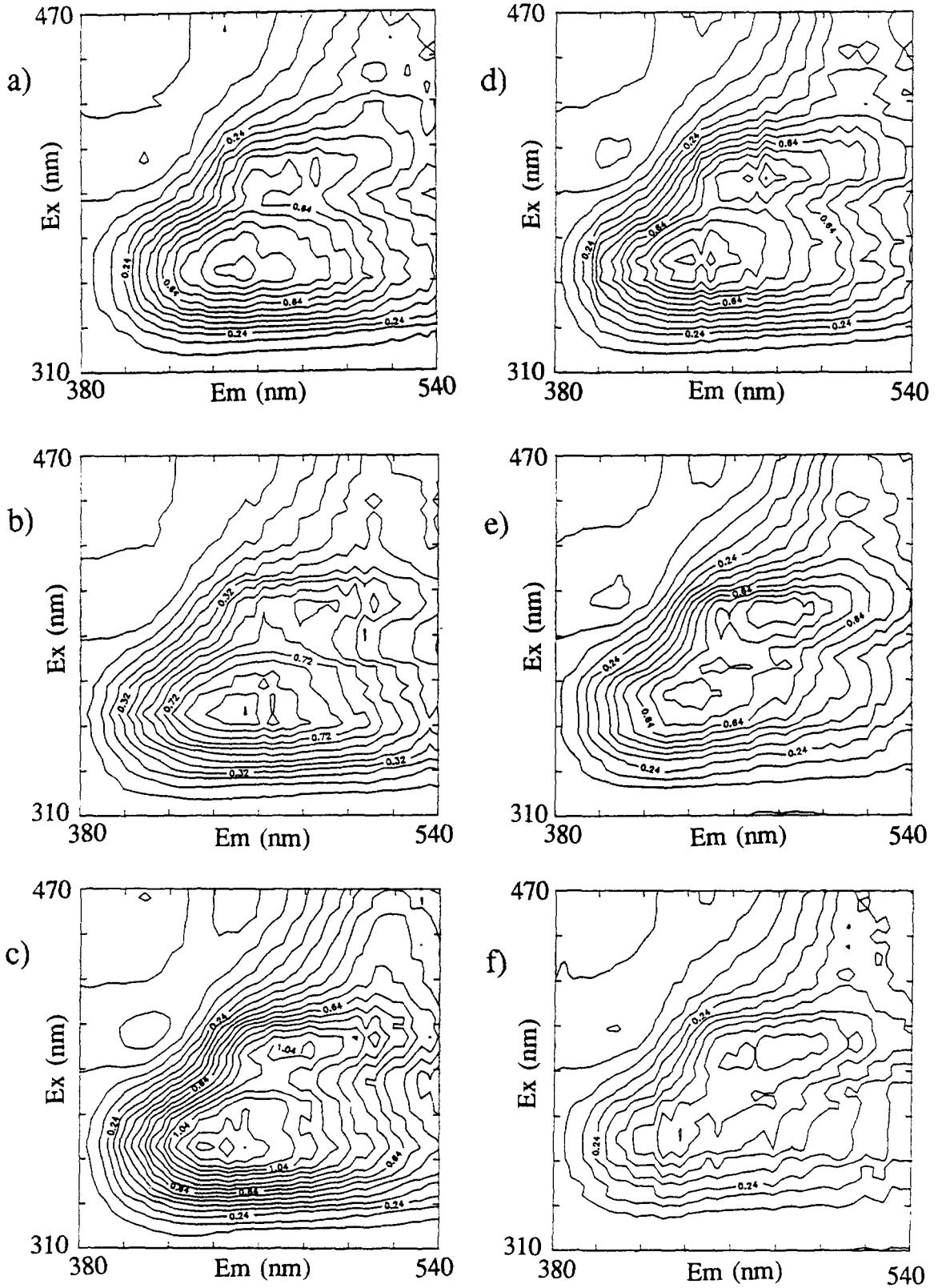

Fig. 3. PREEMs (rank 3 constructions) for NHS at (a) 8 MHz, (b) 10 MHz, (c) 18 MHz, (d) 25 MHz, (e) 85 MHz, and (f) 115 MHz.

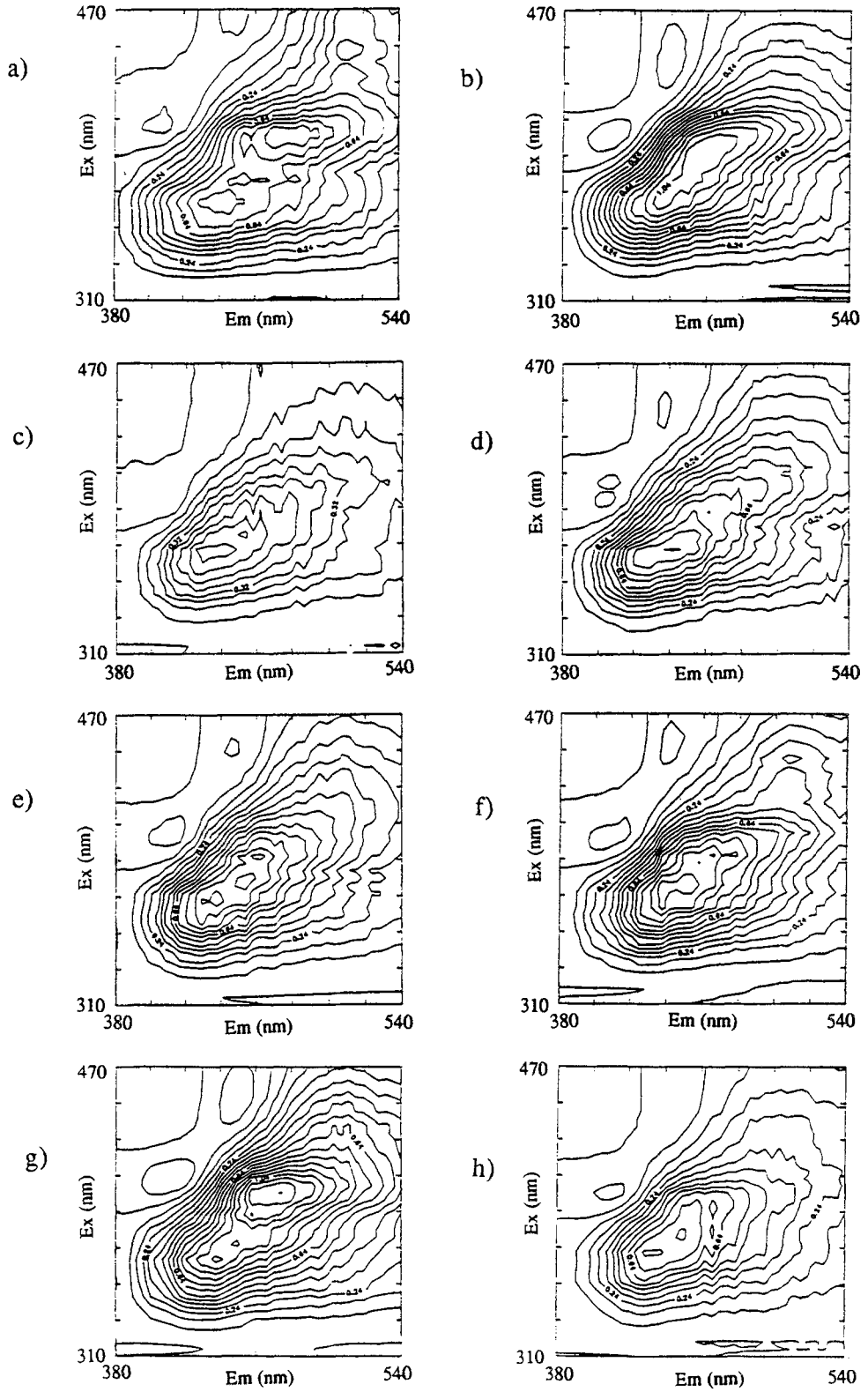

Fig. 4. PREEMs at 85 MHz (rank 3 constructions) of (a) NHS, (b) NHS(ls), (c) TFHS, (d) TFHS(ls), (e) SFHS, (f) SFHS(ls), (g) HHS, and (h) TSHFHS(ls).

good visual discrimination between the different samples. Clearly, the PREEMs show much more variation between samples than did the steady-state EEMs (Fig. 1). Peaks I and II are both evident in NHS. Variations in the other sera range from TFHS, which is dominated by Peak I, to HHS, which is dominated by Peak II. The weaker peak at $\lambda_{ex}=446$ nm, $\lambda_{em}=516$ nm is clearly discernible only in the PREEMs of NHS and SFHS(ls).

In order to compare quantitatively the different sera, both UMCs and Peak I/Peak II intensity ratios were calculated for the steady-state EEMs and the PREEMs. The results are shown in Tables I and II, respectively. The UMCs were calculated for each type of serum (the "test" serum) with a "standard" sample, which was either NHS or NHS(ls). For NHS, the mean EEMs and PREEMs of the triplicate runs (the first row in Table I) were used as the "standard" matrices. Test samples showing significant differences from the standards are indicated in Table I for 95, 99, and 99.5% confidence levels.

Several observations can be made about the results shown in Table I. First, none of the steady-state EEMs for the test sera are highly correlated with the NHS standard. This is due in part to the presence of a more intense contribution in the EEM of NHS from proteins in the short wavelength region. Small shifts in the position of the dominant peak (see Fig. 1) also contribute to these differences. Most importantly, however, is the observation that the UMCs of the steady-state EEMs are all clustered in the 0.90–0.93 range, offering little discrimination between test sera.

The PREEMs do not contain the short-wavelength protein contributions, due to a cutoff by the phase-modulation optics of transmission below approximately 300 nm. The UMCs of the test PREEMs with the NHS standard PREEMs are therefore higher than for the corresponding steady-state EEMs. Actually, the PREEMs offer better discrimination among the different test sera. While the steady-state UMCs fail to discriminate among TFHS, TFHS(ls), and SFHS, or among SFHS(ls), NHS(ls), and HHS, discrimination is provided for both sets of sera by the PREEMs [at 85 and 115 MHz for TFHS/TFHS(ls)/SFHS and at 10 MHz for SFHS(ls)/NHS(ls)/HHS]. PREEMs at 10 MHz generally afford the best discrimination between the test sera, while 115 MHz provides the most significant differences (all above the 99% confidence level) from the NHS standard sera.

Based on both the UMC values and the confidence tests, TFHS is the most different from NHS and HHS is the most similar to NHS. It is also interesting to note that there is a substantial difference between the UMC for TFHS and that for TFHS(ls), whereas the UMCs of SFHS and SFHS(ls) are almost identical.

The UMCs for the lipid-stripped test sera with the lipid-stripped NHS standard [NHS(ls)] indicate that lipid-stripping greatly reduces the spectral differences among the various sera. Significance levels could not be calculated for the UMCs with NHS(ls) standard because replicate runs were not performed. Several similarities are observed between the UMCs with NHS standard and the UMCs with NHS(ls) standard: the PREEMs offer better discrimination among test sera than do the steady-state EEMs, the best discrimination occurs at 10 MHz, and the testosterone-free serum [TFHS(ls)] is the most unlike the normal serum [NHS(ls)].

The Peak I/Peak II intensity ratios for the various samples are shown in Table II. Standard deviations of the peak ratios were estimated to fall in the range of 0.01–0.09. For all samples, the peak ratios from the PREEMs are much lower than the peak ratios from the steady-state EEMs. This is consistent with the observation that the steady-state EEMs are dominated by the Peak I (Fig. 1). In general, the peak ratios of the lipid stripped sera are greater than those of the non-lipid-stripped sera at the lower modulation frequencies; an exception is NHS(ls), which is almost identical to NHS.

Table II. Peak I/Peak II Intensity Ratios for Various Pooled Sera[a]

	Peak ratio				
Serum	SS	10 MHz	25 MHz	85 MHz	115 MHz
NHS	3.10	1.23	1.07	0.71	0.83
NHS(ls)	2.63	1.24	1.07	0.96	0.85
TFHS	2.98	1.22	1.15	1.28	1.08
TFHS(ls)	3.30	1.70	1.47	1.26	0.98
SFHS	3.15	1.25	1.32	1.07	1.21
SFHS(ls)	2.98	1.10	1.24	1.02	1.12
HHS	2.34	1.11	1.00	0.81	0.80
TSHFHS(ls)	2.96	1.40	1.22	1.12	1.25

[a] Steady-state (SS) EEMs and PREEMs are rank 3 constructions. Standard deviations of ratios in the range of 0.01–0.09.

Modulation Frequency Dependence of UMCs and Peak Ratios

In addition to comparisons between sera at a single modulation frequency, it is also informative to compare the variations of the UMCs and peak ratios with modulation frequency (ω). The UMCs are calculated between the test sera and the NHS or NHS(ls) standard sera; invariance of the UMCs with modulation frequency therefore indicates that the test serum has the same frequency dependence as the standard serum. On this basis, NHS(ls) is the most similar to NHS, and TFHS is the

least similar to NHS. Similar comparisons of the frequency dependence of the UMCs for the lipid-stripped test sera with NHS(ls) standard are difficult to make, due to the small range of the variations with frequency.

The frequency dependence of the peak ratio data, shown in Fig. 5, also provides insight into similarities and differences among the various samples. SFHS and SFHS(ls) have essentially identical curves, indicating that lipid stripping causes no difference in the spectral characteristics of SFHS; this is consistent with the similarity between their UMCs (Table I). NHS(ls), TFHS(ls), and HHS form a second group showing similar trends, and NHS and TSHFHS(ls) form a third group. The frequency dependence of TFHS is unique, setting it apart from the other sera. This is consistent with the markedly low correlations between TFHS and NHS (Table I).

Fluorescence Lifetime Data for Normal Human Serum

Fluorescence lifetimes were determined for NHS at four sets of wavelengths ($\lambda_{ex}/\lambda_{em}$): 366/448 nm (Peak I), 398/472 nm (Peak II), 395/495 nm, and 472/516 nm. Table III shows the results for fitting the multifrequency data to one-, two- and three-component models. Based on the chi-square value, which indicates goodness of fit to a model, the two-component and three-component models are clearly better than the one-component model. It is more difficult to compare the relative accuracy of the two- and three-component models. Due to the complexity of serum, it is likely that there are many lifetime components, both discrete and distributions, at a given wavelength; these components arise from the various compounds and their distributions among different binding microenvironments. Interpretation of lifetime data is further complicated by the similarities among the lifetimes that have been reported for different compounds (see below). In light of these difficulties, attempts were not made to fit the data with distributions or larger numbers of components. Instead, we tried only to identify major lifetime groups.

The results indicate four groups of lifetime components: 10^2 ps, 1–2 ns, 4–7 ns, and 9–10 ns. In a study by Miller *et al.* [25], fluorescence lifetimes of pooled human serum were measured by using pulsed excitation at 388 nm and observing the emission response in the range of 435–485 nm. A three-component fit, reported

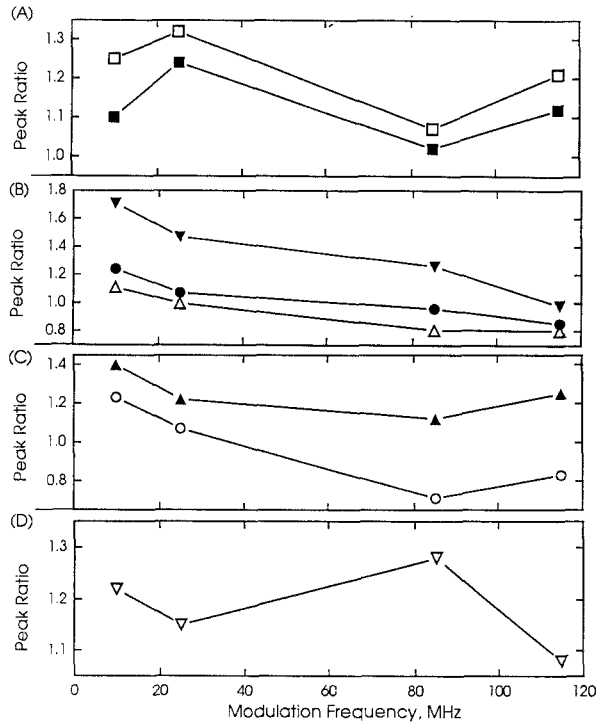

Fig. 5. Peak I/Peak II intensity ratios vs modulation frequency. (A) (□) SFHS and (■) SFHS(ls); (B) (▼) TFHS(ls), (●) NHS(ls), and (△) HHS; (C) (▲) TSHFHS(ls) and (○) NHS; (D) (▽) TFHS.

Table III. Fluorescence Lifetime Data for NHS[a]

One-component fit				
$\lambda_{ex}/\lambda_{em}$ (nm)	τ	χ^2		
366/448	4.4	34		
398/472	1.8	105		
395/495	2.5	61		
472/516	1.0	6.0		
Two-component fit				
$\lambda_{ex}/\lambda_{em}$ (nm)	τ_1 (α_1)	τ_2 (α_2)	χ^2	
366/448	1.2 (40%)	8.9 (60%)	1.2	
398/472	0.59 (39%)	5.6 (61%)	0.92	
395/495	0.85 (43%)	6.8 (57%)	1.4	
472/516	0.46 (66%)	6.5 (34%)	1.4	
Three-component fit				
$\lambda_{ex}/\lambda_{em}$ (nm)	τ_1 (α_1)	τ_2 (α_2)	τ_3 (α_3)	χ^2
366/448	0.15 (10%)	10 (50%)	2.0 (40%)	0.57
398/472	0.49 (36%)	23 (5%)	4.7 (59%)	0.72
395/495	0.36 (24%)	9.8 (34%)	2.6 (42%)	0.41
472/516	0.46 (37%)	6.5 (63%)	—	2.05

[a] Lifetime (τ) in nanoseconds; fractional intensity contributions (α) shown for each lifetime component in two-component and three-component fits; χ^2 is goodness-of-fit parameter and should be close to unity.

Table IV. Uncorrected Matrix Correlations (UMC) for TFHS and TFHS + T with NHS[a]

	UMC[b,c]				
Serum	SS	10 MHz	25 MHz	85 MHz	115 MHz
Standard: NHS					
NHS[d]	0.9987 (±0.0002)	0.9925 (±0.0005)	0.9953 (±0.0005)	0.9896 (±0.0022)	0.9924 (±0.0004)
TFHS	0.9292*** (±0.0009)	0.9454*** (±0.0017)	0.9720*** (±0.0013)	0.9587*** (±0.0044)	0.9638*** (±0.0031)
TFHS + T	0.9413*** (±0.0055)	0.9626*** (±0.0029)	0.9762*** (±0.0016)	0.9749** (±0.0060)	0.9787* (±0.0085)

[a] Steady-state (SS) EEMs and PREEMs are rank 3 constructions, all collected in triplicate.
[b] Mean UMCs ± SD for test EEMs and PREEMs with NHS standard.
[c] Significant difference between test and standard sera indicated by superscript asterisks.
[d] Mean UMCs ± SD, calculated between triplicate EEMs and between triplicate PREEMs of NHS standard.
* At 95% confidence level.
** At 98% confidence level.
*** At 99.9% confidence level.

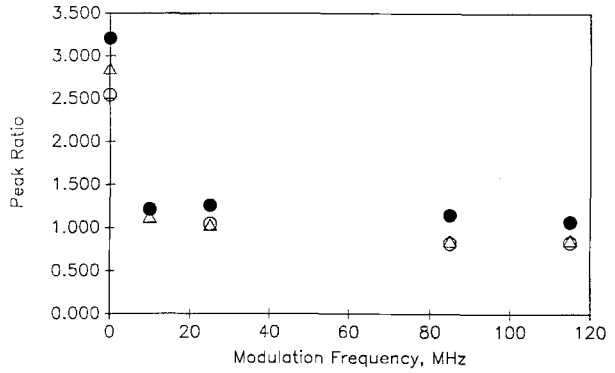

Fig. 6. Peak I/Peak II intensity ratios vs modulation frequency. (○) NHS; (●) TFHS; and (△) TFHS + T.

as weighted averages over the entire emission wavelength range, yielded lifetime components of 0.52, 2.52, and 7.68 ns. These results are more or less consistent with the lifetimes found in this study.

Fluorescence lifetime values have been reported in the literature for several serum components, including values in the 4.0-to 4.5-ns range for pyridoxal, pyridoxal phosphate, and riboflavin, 5.6 ns for FMN, 10.9 ns for 3-hydroxyanthranilic acid [26,27], 30 ps and 1 ns for protein-bound bilirubin and its photoproducts, respectively [24], and a heterogeneous decay with 0.2- and 0.8-ns components for NADH [28,29]. A lifetime of 4.5 ns has also been reported for NADH [27]. Most of these lifetime values can be found in the two-component or three-component fits to our data.

One study has suggested that LDLs are likely to contribute to the visible spectrum of serum over a wide region, due primarily to fluorophores associated with both the lipid and the protein fractions; peaks were tentatively attributed to retinol and vitamin A derivatives, lipid peroxidation products, and aminoiminopropene products formed by reactions between lipid peroxidation products and reactive aldehydes [20]. Further studies are needed in order to identify and characterize the fluorescence lifetime components of LDL.

Addition of Testosterone to Testosterone-Free Serum

An important consideration in studies of the commercial sera that were stripped of particular components is whether the spectral differences between them and the normal sera arise from the absence of the component or from an artifact related to the processing of the serum. We addressed this concern by adding testosterone back to the testosterone-free serum. The TFHS was chosen for this study because it was the most different from NHS. Of course, it is possible that the testosterone might not be incorporated into the serum *in vitro* in the same way that it would be naturally incorporated into the serum *in vivo*. Nevertheless, if the addition of testosterone increases the similarity of the TFHS sample to NHS, it is likely that the differences between TFHS and NHS can be attributed to the removal of testosterone rather than processing artifacts.

Steady-state EEMs and PREEMs at 10, 25, 85, and

115 MHz were collected in triplicate for NHS, TFHS, and TFHS with added testosterone (TFHS + T). In all cases, 50 × 50 matrices were collected over the spectral regions of 310–510 nm for excitation and 380–580 nm for emission.

Examination of the EEMs and PREEMs shows that the addition of testosterone to TFHS does increase its spectral similarity to NHS. For example, Peak II is much less intense in TFHS than in NHS, and the addition of testosterone increases the Peak II intensity. Figure 6 shows the Peak I/Peak II intensity ratios for the EEMs and PREEMs of the three sera as a function of modulation frequency (the steady-state ratios are plotted at zero frequency). In all cases except 10 MHz, there is >98% confidence of a significant difference between TFHS and the other two sera. The confidence level falls to <80% for a significant difference between NHS and TFHS + T, which is a strong indication that the differences between NHS and TFHS are indeed due to the removal of testosterone rather than a processing artifact.

UMCs were also calculated, using TFHS and TFHS + T as the test samples and NHS as the standard sample. Results are shown in Table IV, including standard deviations and confidence levels for significant differences between samples. For all of the EEMs and PREEMs, TFHS + T is more highly correlated with NHS than is TFHS. There is a significant difference between NHS and TFHS at the 99.9% confidence level for all PREEMs and EEMs. For TFHS + T, the confidence decreases to the 98% level at 85 MHz and 95% at 115 MHz, indicating that the addition of testosterone to TFHS increases its similarity to NHS. Moreover, the UMCs of TFHS + T show less variation with modulation frequency than those of TFHS, which means that the frequency dependence of the spectral features of TFHS + T is more similar to that of the spectral features of NHS.

CONCLUSIONS

The purpose of this study was to explore PRFS as a tool for spectral characterization of complex, biological samples. The results illustrate the enhanced spectral discrimination between the various pooled human sera that results from the incorporation of the fluorescence lifetime dimension through PRFS. Both UMCs and peak intensity ratios are useful measures of the similarity, or difference, between samples. In both cases, the PREEMs offer better discrimination between samples than the steady-state EEMs. In general, 10 MHz provided the best discrimination, which suggests that longer-lived luminescent components are responsible for most of the spectral differences. The modulation frequency dependence of the UMCs and peak ratios is a further tool for comparing samples.

The hyperlipid serum (HHS) shows the highest degree of spectral similarity to the normal serum (NHS), and the testosterone-free serum (TFHS) is the least similar. The addition of testosterone to TFHS significantly increases its similarity to NHS, indicating that the spectral differences between the various commercial pooled sera are due to the absence of the removed component rather than a processing artifact. A much greater degree of spectral similarity was observed between the various lipid-stripped sera than between the non-lipid-stripped sera, indicating that lipids do influence the spectral characteristics of serum.

Unlike direct lifetime measurements, PRFS produces a direct measure of intensity that is a function of the spectral characteristics, concentrations, and fluorescence lifetimes of the fluorescent components. Since continuum sources can be used in PRFS without compromising the quality of the lifetime information, it is possible to scan fully excitation wavelength as well as emission wavelength, providing the two independent spectral dimensions in the PREEM format. Like steady-state intensity, PRFI is additive for independently emitting components. The PREEM data may therefore be analyzed by the same techniques that have been well described for steady-state EEM data.

On the instrument used in this work, both steady-state intensity and PRFI are acquired sequentially, one wavelength at a time; collection of a 40 × 40 EEM or PREEM in which each point is the internal average of 10 measurements requires approximately 1 h. The acquisition time could be reduced to the time required for a single intensity measurement by using two-dimensional array detection. Furthermore, recent advances in frequency-domain instrumentation have made it possible to acquire data over a wide range of frequencies in a single measurement, using Fourier transform technology [30]. Extension of this technology to the PRFS technique, in combination with array detection in the spectral domains, would enable the simultaneous, essentially instantaneous, acquisition of the entire excitation–emission—frequency array (EEFA).

An important result of this work is the demonstration that UMCs and peak ratios provide similar discrimination between samples. Thus, the initial collection of full EEFA data could serve as the basis for selection of a much smaller number of discrete features (PRFIs measured at a few wavelengths and modulation frequencies) to use for rapid screening and analysis.

ACKNOWLEDGMENT

This work was supported by the Division of Chemical Sciences, Office of Basic Energy Sciences, Office of Energy Research, United States Department of Energy (Grant DE-FG0588ER13931).

REFERENCES

1. T. T. Ndou and I. M. Warner (1991) *Chem Rev.* **91**, 493–507.
2. O. S. Wolfbeis and M. J. P. Leiner (1985) *Anal. Chim. Acta* **167**, 203–215.
3. M. J. P. Leiner, M. R. Hubmann, and O. S. Wolfbeis, in W. Baeyens, D. deKeukeleire, and K. Korkidis (Eds.), *Luminescence Techniques in Chemical and Biochemical Analysis*, Marcel Dekker, New York, 1990, Chap. 12, pp. 381–419.
4. M. J. P. Leiner, M. R. Hubmann, and O. S. Wolfbeis (1987) *Anal. Chim. Acta* **198**, 13–23.
5. M. J. P. Leiner, R. J. Schaur, G. Desoye, and O. S. Wolfbeis (1986) *Clin. Chem.* **32**, 1974–1978.
6. X. Xu, J. Meng, and S. Hou, (1988) *J Luminesc.* **40/41**, 219–220.
7. T. V. Veselova, A. S. Cherkasov, and V. I. Shirokov (1970) *Opt. Spectrosc.* **29**, 617–618.
8. J. R. Lakowicz and H. Cherek (1981) *J. Biochem. Biophys. Meth.* **5**, 19–35.
9. J. R. Mattheis, G. W. Mitchell, and R. D. Spencer, (1983) in D. Eastwood (Ed.), *New Directions in Molecular Luminescence*, ASTM STP 822, American Society for Testing and Materials, Philadelphia, pp. 50–64.
10. L. B. McGown and D. S. Kreiss (1988) *SPIE Vol. 910 Fluoresc. Detect. II*, pp. 73–80.
11. P. M. R. Hertz and L. B. McGown (1991) *Appl. Spectrosc.* **45**, 73–79.
12. D. W. Millican and L. B. McGown (1989) *Anal. Chem.* **61**, 580–583.
13. L. B. McGown (1989) *Anal. Chem.* **61**, 839A.
14. L. B. McGown and D. W. Millican (1988) *Appl. Spectrosc.* **42**, 1084–1089.
15. K. Nithipatikom and L. B. McGown (1987) *Appl. Spectrosc.* **41**, 1080–1082.
16. G. Weber (1961) *Nature* **190**, 27–29.
17. I. M. Warner (1982) in D. Hercules, G. M. Heiftje, L. R. Snyder, and M. A. Evenson (Eds.), *Contemporary Topics in Analytical and Clinical Chemistry*, Plenum Press, New York, Vol. 4.
18. M. D. Russell and M. Gouterman (1988) *Spectrochim. Acta* **44A**, 857–861.
19. D. S. Burdick, X. M. Tu, L. B. McGown, and D. W. Millican (1990) *J. Chemom.* **4**, 15–28.
20. E. Koller, O. Quehenberger, G. Jurgens, O. S. Wolfbeis, and H. Esterbauer (1986) *Fed. Eur. Biomed. Soc.* **198**, 229–234.
21. G. H. Golub and C. F. Van Loan (1983) *Matrix Computations*, Johns Hopkins University Press, Oxford.
22. X. M. Tu and D. S. Burdick (1989) *J. Chemom.* **3**, 431–441.
23. X. M. Tu, D. S. Burdick, D. W. Millican, and L. B. McGown (1989) *Anal. Chem.* **61**, 2219–2224.
24. C. D. Tran and G. S. Beddard (1982) *J. Am. Chem. Soc.* **104**, 6741–6747.
25. N. A. Miller, S. Gangopadhyay, and W. L. Borst (1988) *SPIE Vol. 909, Time-Resolved Laser Spectroscopy in Biochemistry*, pp. 200–206.
26. W. R. Ware and B. A. Baldwin (1964) *J. Chem. Phys.* **40**, 1703–1705.
27. R. F. Chen, G. G. Vurek, and N. Alexander (1967) *Science* **156**, 949–951.
28. R. D. Spencer and G. Weber (1969) *Ann. N.Y. Acad. Sci.* **158**, 361–376.
29. J. R. Lakowicz and B. P. Maliwal (1985) *Biophys. Chem.* **21**, 61–78.
30. Product information, MHF lifetime instrument, SLM Inc., Urbana, IL.